JOURNAL OF PROPULSION AND POWER
Vol. 16, No. 6, November–December 2000

Comparison of Spray/Wall Impingement Models with Experimental Data

Seong Hyuk Lee* and Hong Sun Ryou†
Chung-Ang University, Seoul 156-756, Republic of Korea

The aim of the study is the comparison of earlier published submodels for the spray impingement and the suggestion of a modified impingement model. The modified model was devised to give better predictions for the upward dispersion of droplets after impingement in diesel engines. The present paper includes two parts, one of which is to analyze the overall structure of impinging sprays and the other to do the internal structure for which the main parameters are the local velocities and mean diameter of droplets. The submodels were investigated to compare the results with the modified model. Numerical results using four different models were compared with several experimental cases for the nonevaporative impinging sprays. As a result, it is found that model 3 and model 4 are acceptable for the predictions of the droplet dispersion normal to the wall.

Nomenclature

D	=	droplet diameter
La	=	Laplace number, defined as $\rho_d \sigma_d D_b / \mu_d^2$
m	=	droplet mass
N	=	number of droplets in a parcel
S_v	=	source term for $\boldsymbol{v}$
t	=	time
t^*	=	time just after which the dome disappears
V	=	total velocity of droplet
$\boldsymbol{v}$	=	velocity vector
We	=	Weber number
$\boldsymbol{x}$	=	position vector
β	=	impinging angle to the normal
ρ_d	=	density of droplet
σ_d	=	surface tension of droplet
$\Omega_{G,(0,1)}$	=	normally distributed random number in the range 0–1
$\Omega_{U,(0,1)}$	=	uniform random number between 0 and 1

Subscripts

a, b	=	after and before impingement, respectively
d	=	droplet
g	=	gas phase
rel	=	relative velocity
t, n	=	tangential and normal directions to the wall, respectively
1, 2	=	identity of two separated droplet parcels

I. Introduction

GENERALLY, it is a well-known fact that the spray–wall interaction problem is very important because the spray impingement is often encountered in a wide variety of field such as spray cooling, ink jet printing, soil erosion by rain, and the direct injection (DI) engines. During the cold starting situation of the DI diesel engines, the fuel-rich zones close to the wall surfaces because of the low gas pressure result in the incomplete combustion with consequently high levels of unburned hydrocarbons and soot particles in the exhaust gases.[1] Therefore, it is necessary to clarify the characteristics of the spray–wall interaction to design more efficient engines and to reduce the emissions.

Actually, computational modeling offers a promising alternative to obtain the detailed information such as the local velocities and Sauter mean diameter (SMD) that are hard to measure in the near-wall region. A number of the numerical submodels for the spray impingement have been developed for describing the interaction between droplets and the wall. Naber and Reitz[2] have proposed a model to study spray impingement using the KIVA code. The main weakness in this model is to ignore the phenomenon of droplet shattering occurring at high collision energy and the loss of momentum and energy of the impinging droplets. Earlier published models that complement the weakness of the preceding model are the submodels proposed by several researchers.[3–6] These models are intrinsically based on the same experimental background as Naber and Reitz's model.[2] In other words, these models described the transition criterion between rebound and wall jet regimes by using the experimental data from Wachters and Westerling[7] on a very hot wall whose temperature is above the Leidenfrost temperature of the fuel. However, the regime criterion used in these models may not be applicable to a wall whose temperature is below the fuel boiling temperature because the appropriate hydrodynamic regime to a cold starting situation in DI diesel engines is the evaporative wetting regime, as argued by several researchers.[5,8,9] Therefore, it is difficult to describe reasonably the splash phenomenon that occurs in a typical cold starting situation. Actually, the interaction between the liquid film deposited on the wall and impinging droplets is important in a typically cold start situation of DI engine, resulting in the splash phenomena. Consequently, the results of these models were found to underpredict significantly the dispersion of sprays away from the wall because of the relatively simple modeling of the reatomization with respect to the diameter and the velocity of the ejected droplets. Therefore, it may be concluded that these models cannot effectively describe the splash phenomenon, which typically occurs in DI diesel engines because there are basically insufficient physical bases on splash mechanism in these models. As efforts to complement these weaknesses, Bai and Gosman,[10] Stanton and Rutland,[11] Mundo et al.,[12] and Senda et al.[8] have proposed the impingement model and showed the improved results for several test cases.

The purpose of the present study is to compare the predictions using the earlier published impingement models with several experimental data to examine the characteristics of numerical models and consequently to suggest a modified model to give better predictions. The submodels of Watkins and Wang,[3] which is referred to as model 1, Park,[6] which is referred to as model 2, and Bai and Gosman,[10] which is referred to as model 3, were investigated to compare with the modified model (model 4). Model 4 was intrinsically based on model 2 and devised to give better predictions for the upward dispersion of droplets after impingement by using the relationships from the experimental results. The numerical simulations

Received 28 August 1998; revision received 28 September 1999; accepted for publication 12 October 1999.

*Researcher, Department of Mechanical Engineering, Heuksuk Dong, DongJak Ku.

†Professor, Department of Mechanical Engineering, Heuksuk Dong, DongJak Ku.

using four different submodels were carried out for the nonevaporative impinging sprays on a wetted and cold wall, representing one with the temperature below the fuel boiling point. The present paper consists of two parts, one of which is the overall structure and the other is the internal structure. The main parameters of the overall structure are the radius and height of wall sprays, which are defined as the penetration lengths of wall sprays in the directions tangential and normal to the wall, respectively. Also, the droplet velocity, SMDs and the gas-phase velocities at the local position are taken for the analysis of the internal structure.

As a result, it is found that the predicted radius of wall sprays by model 2 agrees fairly well with the experimental data, whereas the spray height is significantly underpredicted against the experimental data. Model 3 shows less penetration in the tangential direction, although it agrees well with the experimental data for the spray height. Meanwhile, model 4 shows the improved results relative to model 2 for the predictions of the upward dispersion of droplets after impingement.

II. Theoretical Models

A. Computational Fluid Dynamics Models of the Continuous and Dispersed Phase

The gas phase is derived in terms of the Eulerian conservation equations. The code used in this study solves the mass and momentum equations, coupled with the modified k–ε model proposed by Reynolds.[13] The governing equations can be written as follows by using a Cartesian coordinate for the simplification:

$$\frac{1}{\Delta V}\frac{\partial}{\partial t}(\theta\rho\Delta V\phi) + \frac{\partial}{\partial x}(\theta\rho u_g\phi) + \frac{\partial}{\partial y}(\theta\rho v_g\phi) + \frac{\partial}{\partial z}(\theta\rho w_g\phi)$$
$$= \frac{\partial}{\partial x}\left(\theta\Gamma_\phi\frac{\partial\phi}{\partial x}\right) + \frac{\partial}{\partial y}\left(\theta\Gamma_\phi\frac{\partial\phi}{\partial y}\right) + \frac{\partial}{\partial z}\left(\theta\Gamma_\phi\frac{\partial\phi}{\partial z}\right) + S_\phi + S_\phi^d \tag{1}$$

where ΔV is the local incremental volume, ρ denotes the density of the gas phase, ϕ represents momentum, mass, turbulent kinetic energy, and dissipation energy, and θ is the void fraction, indicating the volume fraction occupied by the gas. The diffusion coefficient and source terms of ϕ are represented by Γ_ϕ and S_ϕ. The source terms with subscript d come from interactions with the liquid phase.

The liquid phase is modeled in a stochastic manner as a spray of discrete droplets that can penetrate and interact with the gas phase. The droplet trajectory and momentum equations are written in terms of the droplet positions as follows:

$$\frac{d\boldsymbol{x}}{dt} = \boldsymbol{v}_d \tag{2}$$

$$\frac{d\boldsymbol{v}_d}{dt} = \frac{3}{4}C_d\frac{\rho}{\rho_d}\frac{V_{\text{rel}}}{D_d}(\boldsymbol{v}_g + \boldsymbol{v}_g' - \boldsymbol{v}_d) + S_{v,d} \tag{3}$$

The drag coefficient C_d is determined from Yuen and Chen.[14] Generally, the particle-eddy interaction model used in the present study is based on the model developed by Gosman and Ioannides.[15] In this model, it is thought that a droplet in a turbulent flow experiences a randomly varying velocity field to which it responds according to its inertia. This process is modeled by a stochastic approach, which assumes that as a droplet traverses the turbulent flowfield it interacts in a random way with a sequence of turbulent eddies. The fluctuating velocity within each eddy is isotropic and obeys a Gaussian probability density function. The interaction time is taken to be the smaller of the eddy lifetime and the interaction time required for the droplet to traverse the eddy. The random perturbation is calculated as follows:

$$\boldsymbol{v}_g = (2k/3)^{\frac{1}{2}}\,\text{sign}(XX)\,\text{erfc}^{-1}(XX) \tag{4}$$

where k is the turbulence kinetic energy, XX is a normally distributed random number in the range -1 to $+1$, and $\text{erfc}^{-1}(\,)$ is the inverse complementary error function.

Table 1 Model of Watkins and Wang[3]—model 1

Rebound regime ($We_{bn} < 80$)	Breakup regime ($We_{bn} \geq 80$)
$D_a = D_b$	$D_a = D_b/4$
$N_a = N_b$	$N_a = N_b$
$v_{at} = \sqrt{1 - 0.95\cos^2\beta}\cdot v_{bt}$	$v_{at} = v_{bt}$
$v_{an} = \sqrt{1 - 0.95\cos^2\beta}\cdot v_{bn}$	$v_{an} = 0$

Table 2 Model of Park[6]—model 2

Rebound regime ($We_{bn} < 80$)	Breakup regime ($We_{bn} \geq 80$)
$D_a = D_b$	$D_{a,1} = D_{a,2} = D_b/N_{\text{eject}}^{\frac{1}{3}}$
$v_{at} = v_{bt}$	$v_{f,1} = -v_{f,2} = 0.835\cdot(3.096 - 2\xi)\cdot v_{bn}\cdot\Omega_{U,(0,1)}$
$v_{an} = \sqrt{1 - \kappa\cos^2\beta}\cdot v_{bn}$	$v_{an,1} = v_{an,2} = \sqrt{1 - \kappa\cos^2\beta}\cdot v_{bn}\cdot\Omega_{U,(0,1)}$
$N_a = N_b$	$N_{a,1} = N_{a,2} = N_b\cdot N_{\text{eject}}/2$

Droplets may become unstable under the action of the interfacial forces induced by their motion relative to the continuous phase. The present study incorporates a breakup model widely used for the breakup of liquid droplets in a gaseous stream proposed by Reitz and Diwakar,[16] where two breakup regimes are identified as the bag and stripping breakup. Also, the collision and coalescence model of O'Rourke and Bracco[17] is used in this paper.

B. Submodels for the Spray Impingement

1. Models of Watkins and Wang (1990) and Park (1994): Model 1 and Model 2

Among the adopted models, models 1 and 2 listed in Tables 1 and 2 have been based on the hot wall data.[7] In model 2, the tangential velocity v_f is given by differentiation of the relationship for the radius of the thin front of the droplets around the dome from the experimental results.[7] It is assumed in model 2 that t at which the drop breaks up is given as a function of the time just after the dome disappears, i.e.,

$$t = \xi\cdot t^* = \xi(D_b/v_{bn}) \tag{5}$$

where the coefficient ξ will be mainly a function of v_{bn}. In this model, the value was from 1.0 to 1.28 for low and high velocity, respectively.[6] In particular, it is assumed in model 2 that an incident droplet parcel with a Weber number higher than 80 is separated into two parcels with same diameter and velocity of droplets after impingement. The coefficient for the loss of energy κ is given by fitting the experimental data.[7] The number of droplets after impingement N_{eject} is determined by the experimental data.[9]

According to earlier studies,[5,8–10] the appropriate hydrodynamic regime is the wetting regime for diesel engines, where the normal in-cylinder surface temperature range from 400 to 600 K. Particularly in DI diesel engines the formation of emissions of unburned hydrocarbons and soot particles dominantly occurs in the cold start situation rather than in operating situation because there is incomplete combustion, resulting in the deposit of fuel film formed on the wall surface. Therefore, models 1 and 2 are not suitable for DI diesel engines of the surface temperature below the critical temperature because both models 1 and 2 use the regime criterion based on the experimental data on a nonwetting regime. In addition, neither of these models effectively accounts for partial deposition, film existing at the wall, energy dissipation of the film, and the splash effect because there are no physical bases on the splash mechanism and the transient behavior of film deposited on the wall.

2. Model of Bai and Gosman (1995): Model 3

Contrary to the preceding models, model 3 by Bai and Gosman[10] was based on the conservative law and devised to describe the splash, which is typically observed in DI diesel engines. As shown in Table 3, this model includes three representative regimes: rebound,

Table 3 Model of Bai and Gosman[10]—model 3

Rebound regime ($We_{bn} < 5$)	Deposition regime ($5 \le We_{bn} < We_c$)	Splash regime ($We_{bn} \ge We_c$)
$D_a = D_b$	$D_a = D_b$	$D_{a,1} = \sqrt[3]{0.5 r_m/(N_1 D_b)}$
$N_a = N_b$	$v_{at} = v_{an} = 0$	$D_{a,2} = \sqrt[3]{0.5 r_m/(N_2 D_b)}$
$v_{at} = 5 \cdot v_{bt}/7$	$N_a = N_b$	$N_{\text{eject}} = 5(We_{bn}/We_c - 1)$
$v_{an} = -e \cdot v_{bn}$		

Table 4 Proposed model—model 4

Rebound regime ($We_{bn} < 80$)	Breakup regime ($We_{bn} \ge 80$)
$D_a = D_b$	$D_a^1 = D_a^2 = 0.2 \cdot \Omega_{G,(0,1)} \cdot D_b$
$v_{at} = v_{bt}$	$v_{f,1} = 0.835 \cdot (3.096 - 2\xi) \cdot v_{bn} \cdot \Omega_{U,(0,1)}$
$v_{an} = \sqrt{1 - \kappa \cos^2 \beta} \cdot v_{bn}$	$v_{f,2} = -v_{f,1}$
$N_a = N_b$	$v_{an,1} = v_{an,2} = -0.15 \cdot \Omega_{G,(0,1)} \cdot v_{bn}$
	$N_{\text{eject}} = (D_b/D_a)^3$
	$N_{a,1} = N_{a,2} = N_b \cdot N_{\text{eject}}/2$

adhesion, and splash. In this model, it is assumed that the arriving droplets are formed in a local film because of coalescence in the adhesion regime. The transition criterion between adhesion and rebound is given as a Weber number of 5. In a rebound regime where a Weber number of an incident droplet is smaller than 5, the normal components of droplet velocities are determined by multiplying the restitution coefficient e used by Bai and Gosman[10] as follows:

$$e = 0.993 - 1.76\theta_i + 1.56\theta_i^2 - 0.49\theta_i^3 \tag{6}$$

where θ_i represents the incident angle of impinging droplets measured from the wall surface. The regime criterion between splash and adhesion is determined by using the relationship from the experimental data.[18]

$$We_c = 1320La^{-0.18} \tag{7}$$

where We_c is a critical Weber number that represents the required energy for the splash. The preceding relationship is derived on the assumption that a wetted surface behaves as a very rough dry wall. In the splash regime, the number of secondary droplets N_{eject} is firstly given by the experimental results.[19] The numbers, N_1 and N_2, of two separated parcels are determined by the randomly varying approach. The secondary droplet sizes are given from the mass conservation equation. This model introduces the mass ratio, r_m, to describe the partial contribution of droplets to the liquid film on the wall. The mass ratio is given as follows:

$$r_m = 0.2 + 0.9 \cdot \Omega_{U,(0,1)} \tag{8}$$

The preceding relationship for a wetted wall is allowed to assume values higher than one because splashing droplets may entrain liquid from the wall film, as in experimental observations.[20] In model 3, the secondary velocity components of ejected droplets are determined from the overall energy conservation equation:

$$0.25 m_a \left(V_{a,1}^2 + V_{a,2}^2\right) + \pi \sigma_d \left(N_1 D_{a,1}^2 + N_2 D_{a,2}^2\right) = 0.5 m_b V_b^2 - \left(We_c \pi \sigma_d D_b^2 / 12\right) \tag{9}$$

Therefore, the secondary velocities of droplets are determined by using the preceding relationship and tangential momentum equation. It was assumed that the ejection angle of droplets would randomly be in the range from 5 to 50 deg. More details are documented in Ref. 10.

3. Proposed Model—Modified Park's Model: Model 4

The previous work[6] has shown that model 2 underpredicted the upward penetration of wall sprays, referred to as spray height, because of the lack of dispersion normal to the wall in model 2. The same results were consistently obtained from the several tests in the present work. This may be because model 2 was based on the experimental data of very hot wall whose temperature is above the Leidenfrost one. Hence, it may be thought that the relationship for the normal dispersion of droplets should be modified in model 2 for better predictions of the splash phenomena. Nevertheless, model 2 shows that the tangential penetration of wall sprays, referred to as spray radius, is predicted better than the other models.

Model 4 is proposed in the present study, and can be regarded as a modified version of model 2 by Park.[6] Model 4 was devised to describe effectively the splashing motion of droplets on the basis of the previous experimental results.[4,9] The main difference between the original Park model (model 2) and the modified Park model (model 4) is in the determination of the normal velocity component of secondary droplets and the size of droplets. Model 4 is based on the hybrid approach coupling model 2 and the relationship from the experimental results[4] from which the normal velocity component and the size of secondary droplets after impingement are determined as shown in Table 4. The numeric constants, 0.15 and 0.2, are given by the experimental results.[4]

III. Computational Details

The gas phase is derived in terms of the Eulerian conservation equations and turbulent transport is modeled by the modified k–ε model.[13] To couple between the gas-phase velocity and the pressure field, the implicit and noniterative PISO algorithm is used in the present study. The gas-phase transport equations are discretized by finite volume method. With this process, the Euler implicit method is used for the transient term, and a hybrid upwind/central difference scheme is used to approximate the convection and diffusion terms. The droplet parcel equations of trajectory, momentum, mass, and energy are written in Lagrangian form. The ordinary differential Lagrangian equations for the droplets are also discretized in the Euler implicit manner.

To demonstrate the usefulness of four different submodels used in the present work, we performed the numerical simulations for four different cases as listed in Table 5. The present work includes two parts, one of which is to analyze the overall structure of impinging sprays and the other to do the internal structure for which the main parameters are the local velocities and mean diameter of droplets. The tests 1–3 seen in Table 5 were taken for the analysis of overall structure of wall sprays and, as a final case, test 4 was adopted for the analysis of internal structure.

Generally, the spray consists of a "main jet region" and a "mixing flow region." The former region lies in the inside of the spray and the latter region extends in the fully developed spray. However, in a small DI engine, the distance between the wall and the nozzle is not long enough to develop the spray fully. The previous research has showed that the model, which assumes that the liquid is already atomized at the nozzle exit, may be inappropriate for high velocity and high gas density.[16] Hence, for the test cases 1–3, we used the model by Reitz and Diwakar[16] to describe effectively the breakup process of liquid jets at the nozzle exit. Reitz[21] applied the wave stability atomization theory to diesel spray modeling by injecting parcels of liquid in the form of "blobs" that have a characteristic size equal to the nozzle hole diameter, instead of assuming an intact liquid at the nozzle exit. The basis of this model is the concept introduced by Reitz and Diwakar[16] that atomization of the injected liquid and the subsequent breakup of droplets are indistinguishable processes within a dense spray.

However, the preceding model may cause the impinging droplet size to be exaggerated for impinging sprays with the low gas density like test 4 (Ref. 16). Hence, it is assumed in the present study that the initial size of droplets can be determined from a Gaussian distribution with the mean diameter of 40 μm obtained from experimental results[22] because there are no relevant information about the initial droplet size distribution. The value of 40 μm is the SMD at the centerline of the free spray at a 30-mm distance from the nozzle exit.

The schedules of injection velocity for the tests 1, 2, and 4 were determined by the curve-fitted relationship from the experimental data produced by Katsura et al.[23] and Arcoumanis and Chang.[22]

Table 5 Specifications of test cases

Test cases	Overall structure			Internal structure
	Test 1 (Ref. 23)	Test 2 (Ref. 23)	Test 3 (Ref. 24)	Test 4 (Ref. 22)
Wall distance, mm	24	34	25	30
Gas pressure, bar	15	15	2	1
Gas temperature, K	293	293	293	293
Nozzle diameter, mm	0.3	0.3	0.25	0.22
Injection pressure, bar	140	140	300	260
Injection duration, ms	1.2	1.2	2.85	1.0
Fuel injected, mm^3/pulse	10.5	10.5	35	4.0

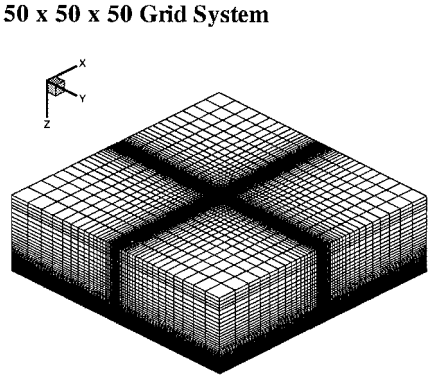

Fig. 1 Computational domain for tests 1 and 2.

However, the velocity schedule for test 3 was assumed by constant velocity based on the experimental condition because there is no information of the velocity schedule in the Ref. 24.

Generally, the preliminary work is required to ensure that the numerical solutions are independent of the used grid systems and the number of introduced droplet parcels, which may affect the numerical solutions. As examining the independence of the preceding parameters on the solutions, the appropriate grid systems and the number of droplets for the statistically independent solutions were chosen for four test cases in the present work. In the case of tests 1 and 2, for example, we performed the numerical simulations using grids of $20 \times 20 \times 20$, $40 \times 40 \times 40$, $50 \times 50 \times 50$, and $60 \times 60 \times 60$ in the x, y, and z directions, respectively. The result was that the grid of $50 \times 50 \times 50$ gave almost the same solution as the grid of $60 \times 60 \times 60$. Figure 1 shows the computational grid system for tests 1 and 2 adopted for the present work. Besides, the numerical simulations were carried out using the total numbers of droplets in the range of from 4800 to 30,000, and consequently it was found that the total number of 18,000 droplet parcels produced almost invariant solutions, compared to the solution of the number of 30,000. In particular, the number of droplets for invariant solutions was taken as 30,000 in the case of test 4 for the analysis of internal structure. For all test cases, a time step of 10 μs was given as the input of simulation. Computing time is about 2.4 h for test 4 using CRAYC90.

IV. Results and Discussion

A. Overall Structure of Wall Sprays (Tests 1–3)

To begin with, we analyze the overall structure of wall sprays, i.e., radius and height of wall spray, for the high gas density. Katsura et al.[23] conducted experiments in which a single spray has normally impinged on a flat plat at high pressure and room temperature of the ambient gas. Figure 2 shows the predicted spray patterns for test 1 at 0.6 ms after injection start. The results of models 1 and 2 show that the secondary droplets mainly leave tangent to the wall surface, and only few droplets are dispersed in the upward direction. On the other hand, model 3 predicted that the splashing droplets due to impingement disperse in both upward and tangential directions after impingement. Model 4 proposed in the present study shows a similar

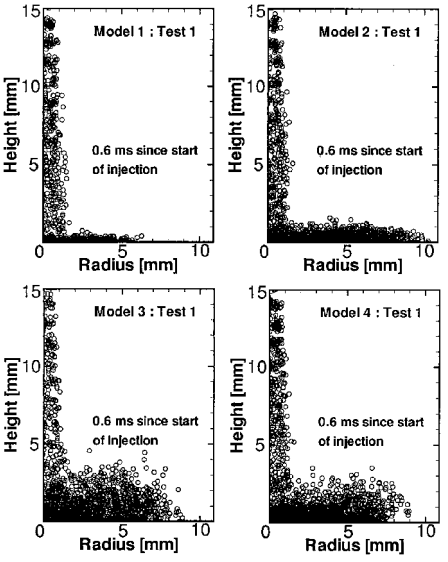

Fig. 2 Calculated spray patterns for test 1.

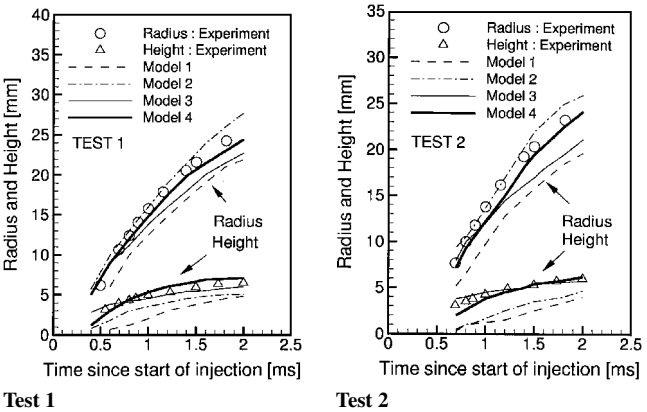

Test 1 **Test 2**

Fig. 3 Spray radius and height.

trend to model 3. The predicted radius and height of wall sprays for tests 1 and 2 were compared with the experimental data,[23] as shown in Fig. 3. The computed radius and height of wall sprays are defined as the penetration lengths of wall sprays in the directions tangential and normal to the wall, respectively. There are some discrepancies among the experimental results, model 1 and model 2. In particular, considerable disagreements are found near the early stage of injection start, indicating that models 1 and 2 cannot predict the upward dispersion of splashing droplets effectively. The reason for the underpredicted upward dispersion is that models 1 and 2 are identically based on the experimental data of Wachters and Westerling[7] for the hot wall whose temperature is above the Leidenfrost temperature of the fuel. According to their experimental observation, a single droplet impinging on the hot wall moves in the tangential direction in the manner of a wall liquid jet for Weber number higher than 80. However, as pointed out by Mundo et al.,[25] the impinging droplets with a Weber number higher than 80 may splash into some secondary droplets. In particular, the splash phenomena is very important for the cold start situation in which the unburned film is formed on the cold wall whose temperature is below the boiling point of the fuel. Therefore, for the case of the wetted and cold wall, it is not consistent to use the preceding criterion coming from the experimental results.[7] As shown in Fig. 3, the disagreement of height is gradually reduced toward the later stage of injection. This is not because models 1 and 2 effectively predict the upward dispersion of secondary droplets, but because there are interactions between the wall-jet vortex and the droplets. On the other hand, model 3 was devised to be capable of predicting the splash phenomena by using experimental results suitable for the cold and wetted wall. Model 4 can be regarded as a modified version of model 2 by adding the

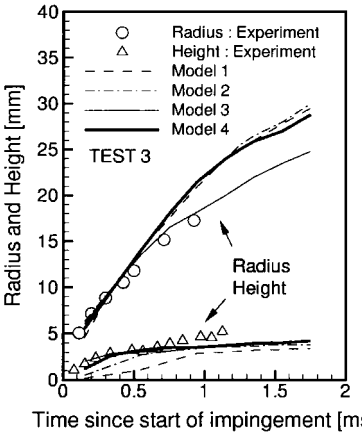

Fig. 4 Spray radius and height (test 3).

upward dispersion terms to the model 2. These models are in better agreements for the height with the experimental data than models 1 and 2, indicating that models 3 and 4 for tests 1 and 2 are acceptable for the prediction of the upward dispersion.

It can be observed that at the early stage after start of impingement, models 2 and 3 are in better agreement for spray radius with experimental data than model 1. However, compared to model 2, model 3 underpredicts the spray radius at the later stage of injection. This discrepancy is larger toward the end of the injection duration. The reason why the radial penetration of model 2 can be closer to experimental data may be the underpredicted normal velocity, resulting in producing smaller ejection angle. Compared with model 3, model 4 produced the improved results of spray radius and height, suggesting that the model 4 is acceptable for the prediction of wall sprays. Actually, the only difference between test 1 and test 2 is in the impingement distance as listed in Table 5. From Figs. 3a and 3b, we can see the effect of the impingement distance on the spray height and radius. Consequently, the growth of the spray radius lessens as the impingement distance increases, indicating that it takes longer to reach the wall prior to impingement.

Figure 4 presents the predicted results for test 3 listed in Table 5. As a similar trend to tests 1 and 2, considerable underprediction of spray height was seen near the early stage of start of impingement and the disagreements are gradually reduced because of the same reason as mentioned in tests 1 and 2 previously. Although there are slight discrepancies among the experimental data, model 3 and model 4, these models perform well in predicting the upward dispersion of droplets after impingement. Compared to model 2, model 4 shows the improved results for the height, indicating that model 4 performs better than model 2 in predicting the splash effect. Generally, the best model prediction for the radius was for model 3. However, all models except model 3 overpredicted the radius after 0.7 ms since start of impingement. In particular, in predicting the radius, it is seen that the result of model 4 is nearly identical to that of model 2 despite that model 4 includes the splash effect. It may be the limits of model 4 because this model is intrinsically based on model 2. Hence, the more elaborated and fundamentally based model is clearly required to give better predictions for nearly all aspects of various situations. Nevertheless, it is thought that model 4 is useful in predicting the droplet dispersion in the upward direction.

B. Internal Structure of Wall Sprays (Test 4)

The phenomenon of impinging sprays on the wall can be affected by various factors such as atomization at the nozzle exit, the behavior of impinging droplets at the impingement site, and the interaction between turbulent gas-phase flow and the dispersed droplets. These factors are recognized as one of the major parts of the two-phase flow. For the last 10 years, most impingement models have been assessed by comparing the overall structure such as the radius and height of the wall spray with experimental data. However, it is important to analyze the internal structure, i.e., droplet velocities, SMD, and velocities of the gas-phase flow to give better understanding of the interaction between the gas-phase flow and the dispersed droplets. Arcoumanis and Chang[22] have investigated the spatial and temporal characteristics of transient diesel sprays impinging on unheated and heated wall using a phase doppler anemometer.

Figure 5 shows the measuring locations, corresponding to representative regions of the two-phase wall-jet: the main wall-jet region (1), the stagnation region (2), and the downstream region (3). According to Katsura et al.,[23] the main wall-jet region lies in the inside of the impinged part, where the tangential velocity and momentum of the droplets are large. Also, in the stagnation region that lies in the edge of the impinged part, droplets at the peripheral region are pushed out to the upper side, and then stagnate in this region and are overtaken by droplets near the wall. In the downstream region, wall-jet vortex can be observed, and turbulent mixing between the droplets and surrounding gas occurs strongly. In the present study, only the main wall-jet near the wall and stagnation region are discussed because regions (1) and (2) are mainly affected by the impingement model, whereas the region (3) may be much more affected by interaction between the turbulent flow and droplets than the impingement model.

Figure 6 presents the predicted tangential velocities of droplets in the main wall-jet region ($H = 0.5$ mm) and near the stagnation region ($H = 5.0$ mm). According to the experimental observations,[22] the droplet tangential velocity in the near-wall region are not settled to a quasi-steady state within the whole injection duration, contrary to those in the stagnation region. Also, the mean velocity generally decreases as the distance from the wall surface increases, suggesting that most of the droplet tangential momentum remains concentrated in the region near the wall surface. It is seen in Fig. 6 that all models are in good agreement with the experimental observations just mentioned.

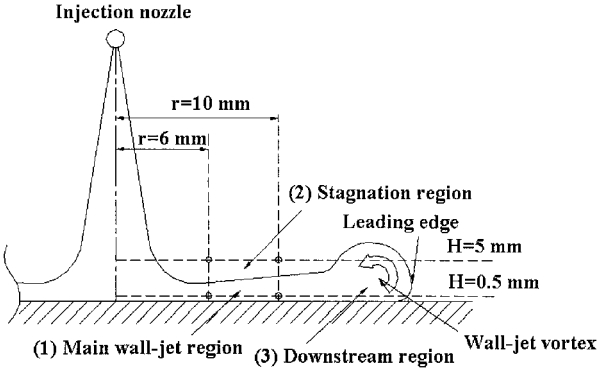

Fig. 5 Structure of impinging sprays.

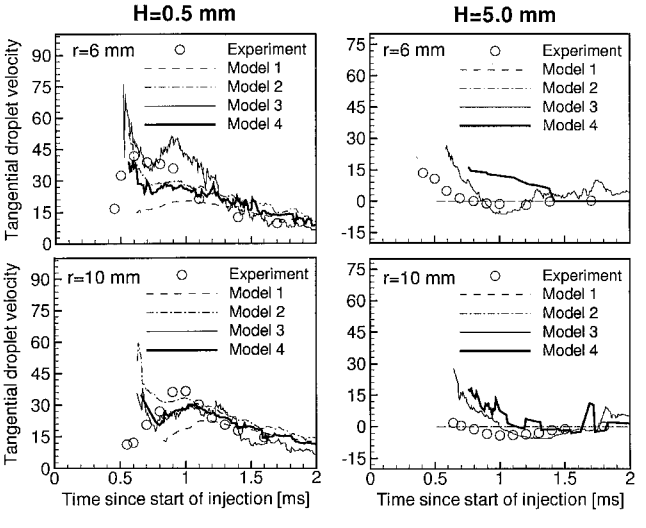

Fig. 6 Comparison of the calculated tangential droplet velocities with the experimental data.

In the main wall-jet region, the results of model 1 are significantly deviated from the experimental data relative to those of the other models. All models except model 1 qualitatively agree well with the experimental trend in that the tangential velocity starts at a maximum and then gradually decays to approximately zero. In particular, it can be found that all models are generally in agreement with the experimental data after 1 ms since start of injection. However, it is difficult to conclude which model shows the best performance for the prediction of droplet tangential velocity. Model 4 proposed in the paper shows a similar trend, compared to the other models.

In the stagnation region, the most outstanding feature is that no results using models 1 and 2 can be found in Fig. 6. This indicates that no secondary droplets at a position in question were detected during the calculation procedure by models 1 and 2 because of the lack of dispersion in the upward direction. This result is consistent with that obtained from the analysis of overall structure as mentioned. In other words, it may be concluded that models 1 and 2 cannot effectively describe the splash effect. Consequently, this problem becomes the main motivation that leads us to modify model 2 in the present work to describe the splash phenomenon.

Contrary to the preceding models, models 3 and 4 successfully captured the presence of droplets in this region because these models were devised to describe the splash effect. Model 3 predicts well the tangential velocity of the droplets near the stagnation region relative to model 4 and also captures the existence of negative tangential velocities, indicating that a wall vortex structure exists in this region, despite the overpredicted velocities at the first stage of injection. However, the actual spray reaches to a quasi-steady state slightly earlier than that predicted by model 3. As seen in Fig. 6 there are considerable deviations between the results of model 4 and the experimental data at $r = 6$ mm and $H = 5$ mm. Nevertheless, model 4 shows the improved results in the stagnation region relative to model 2 in that the model predicts the existence of droplets in this region. It is thought that models 3 and 4 are generally effective to predict the droplet tangential behavior. Meanwhile, model 3 produced the best predictions for the droplet tangential velocity.

Figure 7 is the comparison of the SMDs in the main wall-jet and stagnation regions. Arcoumanis and Chang[22] have argued that there are some fluctuating curves at $r = 10$ mm and $H = 0.5$ mm during the whole injection period different from those upstream of the wall-jet, caused by the outcome of the competitive process between droplet breakup and coalescence. All models underpredict the SMD relative to the experimental data because of the breakup and coalescence model near the wall and inappropriate size distribution of droplets after impingement. However, in the stagnation region, the predicted SMDs by models 3 and 4 are in fairly good agreement except at the first stage of injection, compared to those of models 1 and 2. Models 1 and 2 entirely fail to predict the existence of ejected

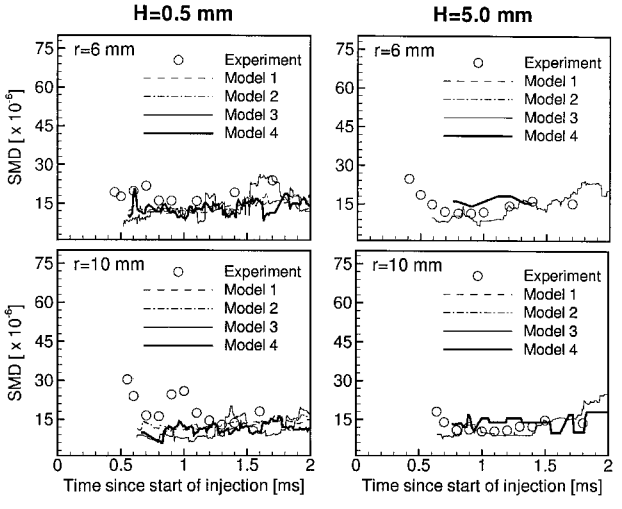

Fig. 7 Comparison of the calculated SMDs with the experimental data.

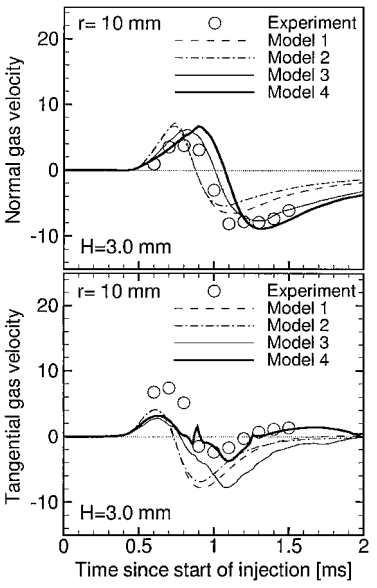

Fig. 8 Comparison of the calculated normal and tangential velocities of the gas-phase with the experimental data.

droplets in the stagnation region. This is because models 1 and 2 significantly underpredict the normal velocities of droplets after impingement, indicating that these models cannot describe the characteristics of the droplet dispersion in the normal direction. Actually, in the submodel for the impingement, the SMDs may be mainly affected by the sizes of ejected droplets and the ejected droplet velocity normal to the wall. Hence, it may be thought that more appropriate modeling for the sizes and normal velocities of ejected droplets is required. Model 4, proposed to overcome this weakness, predicts the existence of droplets and shows the improved results for the SMDs in the stagnation region.

Figure 8 compares the magnitude of normal and tangential velocities of the gas-phase flow at $r = 10$ and 3.0 mm (near stagnation region). In Fig. 8, the positive direction for the normal velocity is defined as the direction away from the wall. Physically, the existence of the region of negative velocities indicates that the surrounding gas is entrained into the main wall-jet region. Hence, the time changing the velocity magnitude to a negative value is very important to analyze the temporal behavior of wall-jet vortex near the wall. The predicted time by model 3 is closer to the experimental data than that of the other models. In particular, the predicted time by models 1 and 2 is faster than that measured because of the lack of the upward dispersion. Hence, it may be thought that the vortex predicted by model 3 moves slower than that predicted by models 1 and 2. This might be because model 3 overpredicted the ejection angle, which was randomly chosen in the range from 5 and 50 deg. After 1.2 ms, it is seen that models 3 and 4 are in better agreement with the experimental data than models 1 and 2.

The predicted tangential velocities by all models except model 4 are approaching zero earlier than results of the experiment. This means that models 1 and 2 overpredict the rotational speed of head vortex at a point in question at the early stage of injection. This is probably because of lack of dispersion further away from the wall in models 1 and 2, which suggests that the ejection angle after impingement is so small that the penetration is overpredicted outward in the radial direction and then, near 0.8 ms at the early stage of injection, the rotational speed is faster than that measured. Although model 3 shows a similar trend to the experimental one, this model overpredicts the negative tangential velocity considerably. Also, it can be noted that after 1.3 ms all models except model 4 fail to predict that the tangential velocity becomes positive, indicating that during the last injection period, the rotational speed of the actual flow is faster than that predicted by models 1–3. As seen in Fig. 8, model 4 performs better than the other models in predicting tangential velocities of the gas-phase flow.

V. Conclusions

The numerical results using the earlier published models and the proposed model (model 4) have been compared with the experimental data. Model 4 was devised to complement the weaknesses of model 2 and to embody physically the splash mechanism by using the relationships from the experimental results. As a result, models 1 and 2 underpredicted the spray height because of the lack of the upward dispersion and, for test 4, none of these models captures the presence of the ejected droplets in the stagnation region. Consequently, it is indicated that models 1 and 2 could not account for the physics of the splash phenomenon. Meanwhile, model 3 produced better prediction of the spray height, although there were some errors in predicting the spray radius. For the internal structure, model 3 is also in good agreement with the experimental data. This is because model 3 was based on the conservation law and devised to be capable of describing the splash phenomena. Model 4 captured the existence of ejected droplets in the stagnation region and showed the similar trend to model 3, indicating that it produced the improved results for the normal dispersion of droplets after impingement, relative to model 2. Additionally, models 3 and 4 have made relatively good predictions of the mean gas-phase velocities. Through the preceding analysis, it can be concluded that models 3 and 4 perform better than models 1 and 2 in predicting the splash effect of impinging sprays on a wetted and cold wall. Nevertheless, there is a clear need for more of a fundamentally based model of nearly all aspects of droplet impingement.

Besides, some discrepancies, which appear in the present study, may be attributed to the turbulence model and particle-eddy interaction model used in the calculation. Actually, the flow of impinging jet can be characterized as a type of flow with the anisotropy of turbulent intensities because of the wall-proximity effect. Nevertheless, most researchers have overlooked this effect, which affects the particle-eddy interaction model. Hence, together with the impingement modeling, it may be an important issue to investigate the effects of turbulence models and the particle-eddy interaction models on the impinging sprays.

References

[1]Gonzalez, M. A., Borman, G. L., and Reitz, R. D., "A Study of Diesel Cold Starting Using Both Cycle Analysis and Multidimensional Calculations," Society of Automotive Engineers Paper 910180, 1991.

[2]Naber, J. D., and Reitz, R. D., "Modeling Engine Spray/Wall Impingement," Society of Automotive Engineers Paper 880107, 1988.

[3]Watkins, A. P., and Wang, D. M., "A New Model for Diesel Spray Impaction on Walls and Comparison with Experiment," *COMODIA 90 Proceedings of International Symposium on Diagnostics and Modeling of Combustion in Internal Combustion Engines*, The Japan Society of Mechanical Engineers, Kyoto, Japan, 1990, pp. 243–248.

[4]Guerrassi, N., and Champoussin, J. C., "Experimental Study and Modeling of Diesel Spray/Wall Impingement," Society of Automotive Engineers Paper 960864, 1996.

[5]Eckhause, J. E., and Reitz, R. D., "Modeling Heat Transfer to Impinging Fuel Sprays in Direct-Injection Engines," *Atomization and Sprays*, Vol. 5, No. 2, 1995, pp. 213–242.

[6]Park, K., "Development of a Non-Orthogonal-Grid Computer Code for the Optimization of Direct-Injection Diesel Engine Combustion Chamber Shapes," Ph.D. Dissertation, Dept. of Mechanical Engineering, Univ. of Science and Technology in Manchester, England, UK, 1994.

[7]Wachters, L. H. J., and Westerling, N. A. J., "The Heat Transfer from a Hot Wall to Impinging Water Drops in a Spherical State," *Chemical Engineering Science*, Vol. 21, No. 11, 1966, pp. 1047–1056.

[8]Senda, J., Kanda, T., Al-Roub, M., Farrell, P. V., Fukami, T., and Fujimoto, H., "Modeling Spray Impingement Considering Fuel Film Formation on the Wall," Society of Automotive Engineers Paper 970047, 1997.

[9]Naber, J. D., and Farrell, P., "Hydrodynamics of Droplet Impingement on a Heated Surface," Society of Automotive Engineers Paper 930919, 1993.

[10]Bai, C., and Gosman, A. D., "Development of Methodology for Spray Impingement Simulation," Society of Automotive Engineers Paper 950283, 1995.

[11]Stanton, D. W., and Rutland, C. J., "Modeling Fuel Film Formation and Wall Interaction in Diesel Engines," Society of Automotive Engineers Paper 960628, 1996.

[12]Mundo, C., Sommerfeld, M., and Tropea, C., "On the Modeling of Liquid Sprays Impinging on Surfaces," *Atomization and Sprays*, Vol. 8, No. 6, 1998, pp. 625–652.

[13]Reynolds, W. C., "Modeling of Fluid Motions in Engines—An Introductory Overview," *Combustion Modeling in Reciprocating Engines*, edited by J. N. Mattavi and C. A. Amann, Plenum Press, New York, 1980, pp. 41–68.

[14]Yuen, M. C., and Chen, L. W., "On Drag of Evaporating Liquid Droplets," *Combustion Science and Technology*, Vol. 14, No. 4, 1976, pp. 147–154.

[15]Gosman, A. D., and Ioannides, E., "Aspects of Computer Simulation of Liquid-Fuelled Combustors," *Energy*, Vol. 7, No. 6, 1983, pp. 482–490.

[16]Reitz, R. D., and Diwakar, R., "Structure of High-Pressure Fuel Sprays," Society of Automotive Engineers Paper 870598, 1987.

[17]O'Rourke, P. J., and Bracco, F. V., "Modeling of Drop Interactions in Thick Sprays and a Comparison with Experiment," *Stratified Charge Automative Engine Conference*, IMechE Conference Publications, London, 1980, pp. 101–116.

[18]Stow, C. D., and Hadfield, M. G., "An Experimental Investigation of Fluid Flow Resulting from the Impact of a Water Drop with an Unyielding Dry Surface," *Proceedings of the Royal Society of London, Series A*, Vol. 373, No. 1755, 1981, pp. 419–441.

[19]Stow, C. D., and Stainer, R. D., "The Physical Products of a Splashing Water Drop," *Journal of the Meteorological Society of Japan*, Vol. 55, No. 5, 1977, pp. 581–531.

[20]Mutchler, C. K., "The Size, Travel and Composition of Droplets Formed by Water Drop Splash on Thin Water Layers," Ph.D. Dissertation, Dept. of Agricultural Engineering, Univ. of Minnesota, 1970.

[21]Reitz, R. D., "Modeling Atomization Processes in High-Pressure Vaporizing Sprays," *Atomisation and Spray Technology*, Vol. 3, No. 4, 1987, pp. 309–337.

[22]Arcoumanis, C., and Chang, J. C., "Flow and Heat Transfer Characteristics of Impinging Transient Diesel Sprays," Society of Automotive Engineers Paper 940678, 1994.

[23]Katsura, N., Saito, M., Senda, J., and Fujimoto, H., "Characteristics of a Diesel Spray Impinging on a Flat Wall," Society of Automotive Engineers Paper 890264, 1989.

[24]Saito, A., Kawamura, K., Watanabe, S., Takahashi, T., and Tuzuki, N., "Analysis of Impinging Spray Characteristics Under High-Pressure Fuel Injection (1st Report, Measurements of Impinging Spray Characteristics)," *Transaction of Japanese Society Mechanical Engineering, Part B.*, Vol. 59, No. 93–0182, 1993, pp. 3290–3295.

[25]Mundo, C., Sommerfeld, M., and Tropea, C., "Droplet-Wall Collisions: Experimental Studies of the Deformation and Breakup Process," *International Journal of Multiphase Flow*, Vol. 21, No. 2, 1995, pp. 151–173.